Journal of Advanced Research 31 (2021) 97–111

Contents lists available at ScienceDirect

Journal of Advanced Research

journal homepage: www.elsevier.com/locate/jare

Fibroblast growth factor 13 stabilizes microtubules to promote Na^+ channel function in nociceptive DRG neurons and modulates inflammatory pain

Qiong Wang [a], Jing Yang [b], Handong Wang [c], Bin Shan [d], Chengyu Yin [e], Hang Yu [c], Xuerou Zhang [c], Zishan Dong [a], Yulou Yu [a], Ran Zhao [a], Boyi Liu [e], Hailin Zhang [a], Chuan Wang [a,*]

[a] Department of Pharmacology, Hebei Medical University, Shijiazhuang 050017, China
[b] Department of Physiology, Hebei Medical University, Shijiazhuang 050017, China
[c] College of Basic Medicine, Hebei Medical University, Shijiazhuang 050017, China
[d] Department of Pharmacy, The Forth Hospital of Hebei Medical University, Shijiazhuang 050017, China
[e] Department of Neurobiology and Acupuncture Research, The Third Clinical Medical College, Zhejiang Chinese Medical University, Key Laboratory of Acupuncture and Neurology of Zhejiang Province, Hangzhou 310053, China

GRAPHICAL ABSTRACT

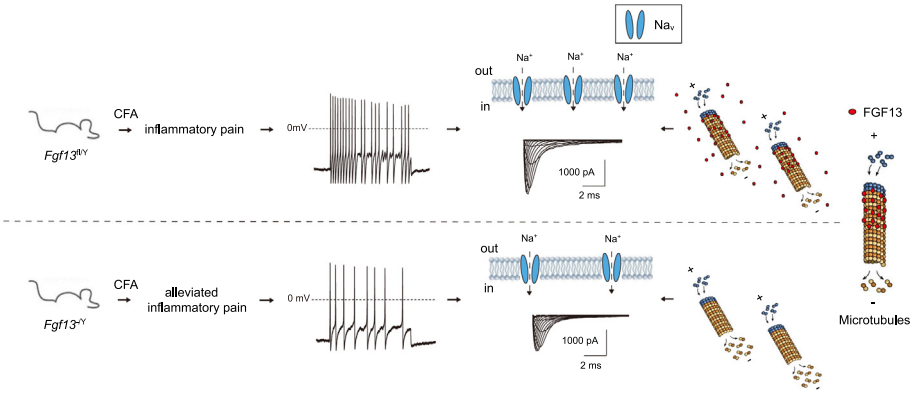

ARTICLE INFO

Article history:
Received 3 September 2020
Revised 16 November 2020
Accepted 14 December 2020
Available online 17 December 2020

Keywords:
Fibroblast growth factor 13
Microtubules
Na^+ channel
DRG
Inflammatory pain

ABSTRACT

Introduction: Fibroblast growth factor homologous factors (FHFs), among other fibroblast growth factors, are increasingly found to be important regulators of ion channel functions. Although FHFs have been link to several neuronal diseases and arrhythmia, its role in inflammatory pain still remains unclear.
Objectives: This study aimed to investigate the role and mechanism of FGF13 in inflammatory pain.
Methods: *Fgf13* conditional knockout mice were generated and CFA-induced chronic inflammatory pain model was established to measure the pain threshold. Immunostaining, western blot and quantitative real-time reverse transcription PCR (qRT-PCR) were performed to detect the expression of FGF13 in CFA-induced inflammatory pain. Whole-cell patch clamp recording was used to record the action potential firing properties and sodium currents of DRG neurons.
Results: Conditional knockout of *Fgf13* in dorsal root ganglion (DRG) neurons ($Fgf13^{-/Y}$) led to attenuated pain responses induced by complete Freund's adjuvant (CFA). FGF13 was expressed predominantly in

Peer review under responsibility of Cairo University.
* Corresponding author at: Department of Pharmacology, Hebei Medical University, 361 East Zhongshan Road, Shijiazhuang, Hebei Province, China.
E-mail address: wangchuan@hebmu.edu.cn (C. Wang).

https://doi.org/10.1016/j.jare.2020.12.009

small-diameter DRG neurons. CFA treatment resulted in an increased expression of FGF13 proteins as well as an increased excitability in nociceptive DRG neurons which was inhibited when FGF13 was absent. The role of FGF13 in neuronal excitability of DRG was linked to its modulation of voltage-gated Na^+ channels mediated by microtubules. Overexpression of FGF13, but not FGF13 mutant which lacks the ability to bind and stabilize microtubules, rescued the decreased neuronal excitability and Na^+ current density in DRG neurons of *Fgf13*$^{-/Y}$ mice.

Conclusion: This study revealed that FGF13 could stabilize microtubules to modulate sodium channel function in DRG neurons and modulate inflammatory pain. This study provides a novel mechanism for FGF13 modulation of sodium channel function and suggests that FGF13 might be a novel target for inflammatory pain treatment.

Introduction

Inflammatory pain can progress into debilitating conditions that dramatically affect the patients' life quality. A large body of evidence suggests that voltage gated sodium channels (VGSCs) are involved in the mechanisms of inflammatory pain [1,2]. Studies have shown that the expression or current densities of VGSCs were up-regulated in nociceptive DRG neurons. The up-regulation of VGSC expression or its activity in peripheral sensory neurons is a crucial step involved in peripheral sensitization, which plays a key role in mediating inflammatory pain. Many pro-inflammatory mediators, including IL-1β or TNF-α are released from local inflammatory sites and up-regulate the expression or activity of VGSCs to promote inflammatory pain [3–6]. However, it remains unclear how VGSC expression or channel activity in nociceptive DRG neurons are modulated under inflammatory pain conditions.

Fibroblast growth factor homologous factors (FHFs), a subfamily of fibroblast growth factors (FGFs), have received increasing attention for their regulation of neuronal VGSCs. Unlike secretory FGFs, FHFs lack the signal peptide for secretion, function intracellularly and do not bind to and activate FGF receptors [7]. There are four members in the FHF family, namly FHF1-4 (with corresponding names to FGF11-14). Many studies have shown that FHFs can bind to the intracellular C-terminal region of the Na_v α subunit to modulate biophysical properties of the channel either in cardiomyocytes [8] or in neurons [9–11]. These effects have been linked to cardiac dysfunction [12–14] and neurodegenerative diseases [15–17]. However, the detailed mechanism of the regulation is still unknown.

Previous study has shown that FGF13 interacts with tubulin and acts as a microtubule-stabilizing protein regulating polarization and migration of cortical neurons during brain development [17]. Several findings suggested that microtubules are involved in the development of pain [18,19]. Microtubule architecture is known to regulate a wide range of cellular processes, including maintenance of cell morphology, mitosis and intracellular transport [20]. Microtubules are the attachment point and repository for a series of proteins and transcription factors in the cell, and form an important intracellular transport pathway assisting the transportation process of proteins and transcription factors [20,21]. Upon microtubule depolymerization, intracellular transportation is suppressed and some functional changes occur in the cell.

In this study, we tested the hypothesis that FGF13 can promote Na^+ channel function through regulating the stability of microtubules in DRG neurons, and thereby participate in inflammatory pain. We found that *Fgf13*$^{-/Y}$ mice showed attenuated response to inflammatory pain. FGF13 expression was significantly increased in DRG neurons of CFA-treated mice. Conditional knockout of *Fgf13* in DRG neurons attenuated the increase in Na^+ channel current density and neuronal excitability in DRG neurons of CFA-treated mice. FGF13 stabilized microtubules to promote Na^+ channel current in DRG neurons. This work revealed that FGF13 could act as a microtubule-stabilizing modulator to promote Na^+ channel current in DRG neurons and further suggested FGF13 might be a novel target for inflammatory pain treatment.

Material and methods

Ethics statement

All animal experiments were approved by the Laboratory Animal Ethical and Welfare Committee of Hebei Medical University (Shijiazhuang, China, Approval No. IACUC-Hebmu-PD-201720) and were in accordance with the International Association for the Study of Pain guidelines for animal use.

Animals

We generated *Fgf13* conditional knockout mice in the DRG via *Cre–loxP*-mediated recombination by mating *Fgf13-loxP* allele (*Fgf13*$^{fl/Y}$ *or Fgf13*$^{fl/fl}$) with a mouse line expressing Cre recombinase under control of the $Na_v1.8$ promoter (*SNS–Cre*) [22]. The *Fgf13-loxP* mice were generated in collaboration with Beijing Biocytogen, Co., Ltd. (Beijing, China) by flanking exon 3 of the mouse *Fgf13* gene with two *loxP* sites [13]. *Fgf13*$^{fl/Y}$; *SNS-Cre* (*Fgf13*$^{-/Y}$) is denoted knockout (*Fgf13* KO) mice. Genomic DNA was isolated from the mouse tail and genotyping was done as described previously [13]. The primers used were as the followings:

PCR for identification of *Fgf13-loxP* gene fragment
5′- TAGTTCCATCTAACAGGGCTCATG (forward)
5′- AGACTTTGGTGGGAGCATCCTG (reverse)
PCR for identification of *Fgf13 Frt* gene fragment
5′-AGTTCGACAGACAGTGCCATTG (forward)
5′- TCTGAACAGATTAGTAATGAACACAGATG (reverse)
PCR for identification of *SNS-Cre* gene fragment
5′-ATTTGCCTGCATTACCGGTC (forward)
5′-GCATCAACGTTTTCTTTTCGG (reverse)

The animals used in our experiments were adult male C57BL/6J mice of 8 weeks to 16 weeks.

*Quantitative real-time reverse transcription PCR (qRT-PCR)*qRT-PCR was performed as we reported [13]. Total RNA was isolated according to the established procedures. Total RNA (1000 ng) was reversely transcribed with PrimeScript™ RT reagent Kit with gDNA Eraser (perfect real time) kit (Takara, Japan) following the manufacturer's instructions. Gene-specific mRNA analyses were performed using the standard protocol of SYBR premix ex Taq™II (TliRnaseH plus) kit (Takara, Japan). *Gapdh* gene was used as a reference gene to normalize the specific gene mRNA expression. After amplification, each qPCR product was sequenced using electrophoresis to ensure the specificity. The primers used are listed in Table 1.

Table 1
List of *qRT-PCR* primer sequences.

Gene name	Primer sequence 5′-3′	Length (bp)
Fgf11	F-CCAAGGTGCGACTGTGCG R-CGACGCTGACGGTAGAGAG	354
Fgf12A	F-CCGCAAGAGGCCAGTGAG R- CACCACACGCAGTCCTACAG	177
Fgf12B	F- GGAGAGCAAAGAACCCCAG R- CACCACACGCAGTCCTACAG	159
Fgf13-core	F- CAGCCGACAAGGCTACCAC R- GTTCCGAGGTGTACAAGTATCC	184
Fgf13S	F- CGAGAAATCCAATGCCTGC R- CACCACCCGAAGACCCACAG	279
Fgf13U	F- GTTAAGGAAGTCATATTCAGAGC R- CACCACCCGAAGACCCACAG	155
Fgf13V	F- GCTTCTAAGGAGCCTCAGC R- CACCACCCGAAGACCCACAG	158
Fgf13VY	F- GCTTCTAAGGTTCTGGATGAC R- CACCACCCGAAGACCCACAG	326
Fgf13VY/Y	F- CACAGAACCCGAAGAGCCTCAG R- CACCACCCGAAGACCCACAG	162
Fgf14A	F- GAGCAGCCCCAGCAAGAAC R- GTGGAATTGGTGCTGTCATC	215
Fgf14B	F- CCCAAATCAATGTGGTTTC R- GTGGAATTGGTGCTGTCATC	211
Gapdh	F- TGTCAGCAATGCATCCTGCA R- CCGTTCAGCTCTGGGATGAC	220

Immunostaining

Standard protocols for fluorescent immunohistochemistry and immunocytochemistry were used as described previously [13,23,24]. The antibodies against FGF13 (1:200, rabbit, Yenzym), NF200 (1:1000, Sigma Aldrich, MO, USA), CGRP antibody (1:1000, Sigma Aldrich, MO, USA), sodium channel (1:1000, Sigma Aldrich, MO, USA), Nav1.7 (1:100, Abcam, Cambridge, United Kingdom) and the correspondent FITC- or Cy3-conjugated secondary antibodies (1:500, Proteintech, USA) were used.

For immunohistochemistry, mice were transcardially perfused with 4% paraformaldehyde (PFA) under terminal anesthesia (sodium pentobarbital, 80 mg/kg). The L4/5 DRG were dissected, post-fixed at 4 °C for 12 h and then transferred in sucrose solution (20% sucrose in PBS) overnight. The following day, tissues were mounted in cryoembedding fluid, frozen, cryosectioned in 10 μm-thick sections and thaw mounted onto slides. Sections of DRG were permeabilized in 3% BSA and 0.3% Triton X-100 (MP biomedicals) for 60 min at 37 °C, and blocked for 30 min at 37 °C with 10% goat serum in PBS. Primary antibodies were diluted in 0.1% Triton X-100/PBS buffer before overnight incubation at 4 °C. After washing three times with PBS, cells were stained with the corresponding FITC- or Cy3-conjugated secondary antibodies for 60 min at 37 °C. All images were collected on a Leica inverted confocal microscope (Model: SP5, Wetzlar, Germany). Images were imported into Photoshop (Adobe) for processing.

For immunocytochemistry, cultured DRG neurons were fixed in 4% PFA for 20 min. Cells were washed three times with PBS and then permeabilized with 0.3% triton X-100 for 60 min at 37 °C. Cells were then incubated with 10% goat serum in PBS for 60 min at 37 °C. Subsequently, cells were incubated overnight with monoclonal anti-sodium channel antibody at 4 °C. After washing three times with PBS, cells were stained with Cy3-conjugated secondary antibody for 60 min at 37 °C. The images were acquired by 3D structured illumination microscopy (3D-SIM) (Nikon, Japan) and analyzed by NIS-Elements Viewer 4.20 software (Nikon, Japan).*Western blot*

Western blot was performed as reported previously [13]. Briefly, ipsilateral L3-L5 DRGs were dissected and then lysed in RIPA buffer [50 mM Tris (pH 7.4), 150 mM NaCl, 1% Triton X-100, 1% sodium deoxycholate, sodium orthovanadate, 0.1% SDS, EDTA, sodium fluoride, leupeptin, and 1 nM PMSF]. Following centrifugation at 12,000 rpm for 30 min, supernatants were collected and protein concentration was quantified using a BCA Protein Assay Kit (Thermo, MA, USA). 50 μg of protein was loaded in each lane. Protein samples were separated on 12% or 15% SDS-PAGE gels and electrophoretically transferred to polyvinyl difluoride (PVDF) membranes (MilliPore, USA). The membranes were blocked with 5% non-fat milk at room temperature for 2 h, followed by overnight incubation at 4 °C with the following primary antibodies diluted in blocking buffer. The antibodies against FGF13 (1:200, Yenzym), Flag (1:1000, Sigma Aldrich, MO, USA), Acetylated α tubulin (Ace-tubulin) (1:800, Sigma Aldrich, MO, USA), Tyrosinated α tubulin (Tyr-tubulin) (1:1000, Millopore, USA), Detyrosinated α tubulin (Detyr-tubulin) (1:1000, Abcam, Cambridge, United Kingdom), α-tubulin (1:2000, Abcam, Cambridge, United Kingdom), β-tubulin (1:2000, Abcam, Cambridge, United Kingdom) and β-actin (1:1000, Bioss, Beijing, China) were used. Subsequently, the immunoblots was incubated with the second antibodies (1: 3000, CST, MA, USA) for 2 h at room temperature. The blots were visualized by the Odyssey Infrared Imaging System (LICOR 9120, Li-COR, USA).

Hot plate test

Mice were placed on a hot plate with the temperature adjusted to 49℃, 52℃ or 55℃ and the cutoff time was 70 s, 50 s or 30 s, respectively. Licking of the hindpaw was considered as a pain behavior signal.

Tail immersion test

The mouse tail was immersed in a water bath at 52℃ or 55℃, and the cutoff time was 15 s or 10 s, respectively.

Hargreaves test

The Hargreaves test was conducted by exposing the plantar surface of the hindpaw to a beam of radiant heat through a transparent surface. The heat stimulation was repeated 3 times for each hindpaw, and the mean withdrawal latency time was calculated.

CFA-induced chronic inflammatory pain model. CFA-induced chronic inflammatory pain model was conducted by a single injection of 20 μL CFA (Sigma Aldrich, MO, USA) into the plantar surface of the hindpaw with normal saline injection as control [25]. Hargreaves test was conducted for three days before injection and at the day 1–7, 10, 14, 21 after induction of inflammation to measure the thermal pain threshold.

DRG neuron culture

DRG neurons were isolated and cultured as described previously [26]. DRGs from 8- to 16-week-old mice were carefully isolated and digested in HBSS basic solution containing collagenase TypeⅡ (2.5 mg/mL) and Dispase (7.5 mg/mL) for 30 min at 37℃. Neurons were cultured with DMEM plus 10% fetal bovine serum.

Electrophysiology

The electrophysiological experiments were performed in small nociceptive neurons (Cm < 42 pF) obtained from L3- L5 DRGs using the whole-cell patch clamp technique as previously described [26]. The voltage and current electrophysiological data were analyzed using Clampfit 10.0, Origin pro 7.5.

Current-clamp recording

Current-clamp recording was performed to record the action potential firing properties of DRG neurons as previously reported [26]. Pipettes (3–4 MΩ) were filled with solution contained (in mM) 140 KCl, 0.5 EGTA, 5 HEPES and 3 Mg-ATP, adjusted to pH 7.3 with KOH. The bath solution contained (in mM): 140 NaCl, 3 KCl, 2 MgCl2, 2 CaCl2 and 10 HEPES, pH 7.3, adjusted with NaOH. A whole cell configuration was obtained at room temperature in voltage-clamp mode with a holding potential of –80 mV and then the recording was performed after switching to current-clamp mode. The data were filtered at 5 kHz and digitized at 20 kHz. Small nociceptive DRG neurons were examined for evoked activity with a series of 1 s current injection from 50 to 500 pA in 50 pA increments. Threshold was determined by the first action potential elicited by a series of depolarizing current injections that increased in 10 pA increments. A hyperpolarizing current injection of 200 ms, −200 pA was used to measure membrane input resistance (Rin), which was assessed from the value of the evoked membrane potential divided by the injected hyperpolarizing current (-200 pA). Linear ramps of currents from 0 to 1000 pA (0.5 s duration) were injected for measuring AP firing parameters.

Voltage-clamp recording

Sodium currents were recorded using the whole cell voltage-clamp technique as previously described [27]. The pipette solution contained (in mM): 70 CsCl, 30 NaCl, 30 TEA-Cl, 10 EGTA, 1 $CaCl_2$, 2 $MgCl_2$, 2 Na_2ATP, 0.05 GTP, 10 HEPES, and 5 glucose, pH 7.3 with CsOH. The bath solution for DRG neurons was (in mM):80 NaCl, 50 choline Cl, 30 TEA-Cl, 2 $CaCl_2$, 0.2 $CdCl_2$, 10 HEPES, and 5 glucose, pH 7.3 with NaOH. The whole-cell configuration was obtained in voltage-clamp mode using an Axopatch 200B amplifier (Molecular Devices). Data was acquired via a Digidata 1322A converter (Molecular Devices). Currents were low-pass filtered at 5 kHz. Voltage errors were minimized with 80%–90% series resistance compensation. The TTX-R sodium current was recorded with additional 300 nm TTX (Abcam, Cambridge, United Kingdom) as external solution. The TTX-S sodium current was obtained by digital subtraction of the TTX-R sodium current from the total current. To isolate $Na_v1.7$ current, 5 nM ProTx-Ⅱ (Abcam, Cambridge, United Kingdom), a selective blocker of $Na_v1.7$,was included in the external solution to inhibit $Na_v1.7$ current [28].

Single cell PCR

We used multi-nested PCR to evaluate the mRNA expression patterns in each DRG neuron tested. After patch-clamp recording, single neurons were collected for single cell PCR. The RT procedures were conducted using GoScript™ Reverse Transcription System kit (Progema, USA) following the manufacturer's instructions. The primes are listed in Table 2.

Adenoviral vector construction

FGF13B or FGF13B$^{S104\text{-}Q111/104A\text{-}111A}$ mutant was cloned into the CMV-MCS-3FLAG-SV40-EGFP vector.

Co-immunoprecipitation (co-IP)

Cells were lysed in buffer containing 25 mM Tris, 150 mM NaCl, 1 mM EDTA, 1% NP40 and 5% glycerol (pH 7.4) with protease inhibitor mixture (Roche, USA) after 48 h of adenovirus infection. The procedures were conducted using Pierce™ Classic Magnetic IP/Co-IP Kit (Thermo, MA, USA) following the manufacturer's instructions. Lysates were centrifuged at 13,000 × g for 10 min at 4 °C and immunoprecipitation was performed with anti-Flag (10 μg, Sigma Aldrich, MO, USA) antibody added to 1000 μg of protein lysates. Samples were rocked overnight, and subsequently incubated with 25 μL of Pierce Protein A/G Magnetic Beads for 8 h at 4 °C, washed three times, Low-pH eluted and boiled in the SDS sample buffer before being subject to SDS-PAGE and immunoblotting.

Table 2
List of single cell PCR primer sequences.

Gene name	Primer sequence 5′-3′	Length (bp)
Scn1a	F_o-CAGAGATGGTGTCGGAGCCT	464
	R_o-CAATGCTCGAAGAACTCTG	
	F_i -TGCCACCTCCGCCCTGTAC	155
	R_i-TTGTCCAGTCGGGAGGGTT	
Scn8a	F_o-CTGCAGAATGAGAAGATGGC	320
	R_o-GTTTTCCCTCTGTTTAATAC	
	F_i-CCTTTCACCCCCGAGTCGCT	184
	R_i-CCAGGCCTTGCGGGATGTC	
Scn9a	F_o-ATGTGAAACAGACCCTGCGT	744
	R_o-ACCCGTATGCCACCCATTTT	
	F_i-TCCTTTATTCATAATCCCAGCCTCAC	134
	R_i-GATCGGTTCCGTCTCTCTTTGC	
Scn10a	F_o-TTCGAAGGCATGAGGGTAGTG	926
	R_o-TAAGAGCGTGGGGGAGAAGT	
	F_i-ACCGACAATCAGAGCGAGGAG	175
	R_i-ACAGACTAGAAATGGACAGAATCACC	
Fgf13	F_o-GAGCCTCAGCTTAAGGGTATAG	335
	R_o-GTTCAGACCTAGATACCACC	
	F_i-CAGCCGACAAGGCTACCAC	185
	R_i-GTTCCGAGGTGTACAAGTATCC	
Gapdh	F_o-AATTCAACGGCACAGTCAA	391
	R_o-TGGGTGGCAGTGATGGCAT	
	F_i-TCGTGGAGTCTACTGGT	192
	R_i-GGGCTAAGCAGTTGGTGG	

F_o, R_o – outer primer pair; F_i, R_i – inner primer pair

Statistical analysis

The results were presented as mean ± SEM. All statistical analyses were carried out with Origin Pro 7.5 software. Student's two-tailed *t* test was used for two group comparisons. One-way ANOVA or two-way repeated-measures (RM) ANOVA was used for multi-group comparisons, followed by Bonferroni *post hoc* test or Dunnett's t *post hoc* test. $P < 0.05$ was considered statistically significant.

Results

Fgf13 conditional knockout mice showed reduced response to inflammatory pain

To determine the function of FGF13 in inflammatory pain, we generated *Fgf13* conditional knockout mice by mating the *Fgf13-loxP* mice with a mouse line expressing *SNS-Cre* recombinase using *Cre-loxP* mediated recombination system. FGF13 expression was greatly reduced in DRG neurons of *Fgf13*$^{-/Y}$ mice as examined by immunohistochemistry (Fig. 1A), immunoblots (Fig. 1B) and qPCR methods (Fig. 1C). We then performed behavioral tests with the control *Fgf13-loxP* mice (*Fgf13*$^{fl/Y}$; Loxp) and the *Fgf13* conditional knockout mice (*Fgf13*$^{-/Y}$; KO). *Fgf13*$^{-/Y}$ mice showed longer latency in hot plate test at 49 °C, 52 °C and 55 °C (Fig. 1D). Similarly, in the tail immersion test at 50 °C and 52 °C, *Fgf13*$^{-/Y}$ mice displayed reduced behavioral responses to noxious thermal stimuli compared with control mice (Fig. 1E). In Hargreaves test, *Fgf13*$^{-/Y}$ mice showed a higher thermal pain threshold compared with *Fgf13*$^{fl/Y}$ mice (Fig. 1F). To investigate whether FGF13 takes part in inflam-

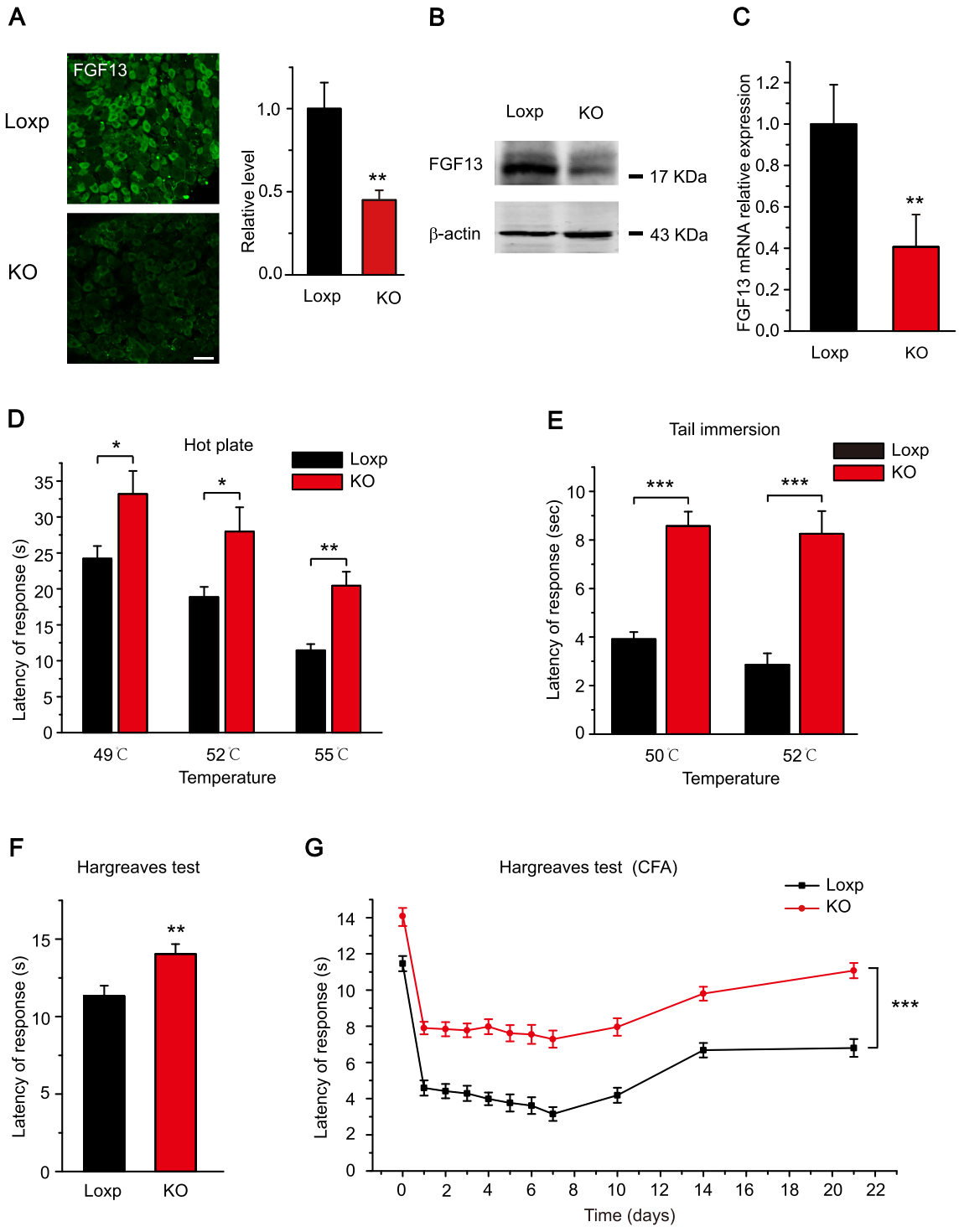

Fig. 1. *Fgf13* conditional knockout mice showed reduced response to inflammatory pain. (A) Representative confocal images of immunostaining of FGF13 in the DRG. FGF13 staining was abolished in *Fgf13* conditional knockout mice. Scale bar: 50 μm. (B) Representative images of FGF13 protein expression in the DRG of Loxp and *Fgf13* KO mice detected by western blot. (C) The mRNA expression levels of FGF13 detected by qPCR. *Gapdh* was used as reference gene. (D) In the hot plate test, the latency responses were increased in $Fgf13^{-/Y}$ mice compared with controls at 49 °C, 52 °C and 55 °C. (E) In the tail immersion test, the latency responses were increased in $Fgf13^{-/Y}$ mice compared with control mice at 50 °C and 52 °C. (F) Response latencies in Hargreaves test. (G) Thermal withdrawal latencies of Loxp and *Fgf13* knockout mice after CFA injection. n = 8 mice/group. $^{*}P < 0.05$, $^{**}P < 0.01$, $^{***}P < 0.001$.

matory pain, we compared the responses of $Fgf13^{fl/Y}$ and $Fgf13^{-/Y}$ mice to CFA-induced chronic inflammatory pain. $Fgf13^{-/Y}$ mice showed reduced responses to thermal pain stimulus (Fig. 1G). Overall, these results indicated that the mice with *Fgf13* conditional knockout in DRG neurons displayed significantly reduced behavioral responses to inflammatory pain.

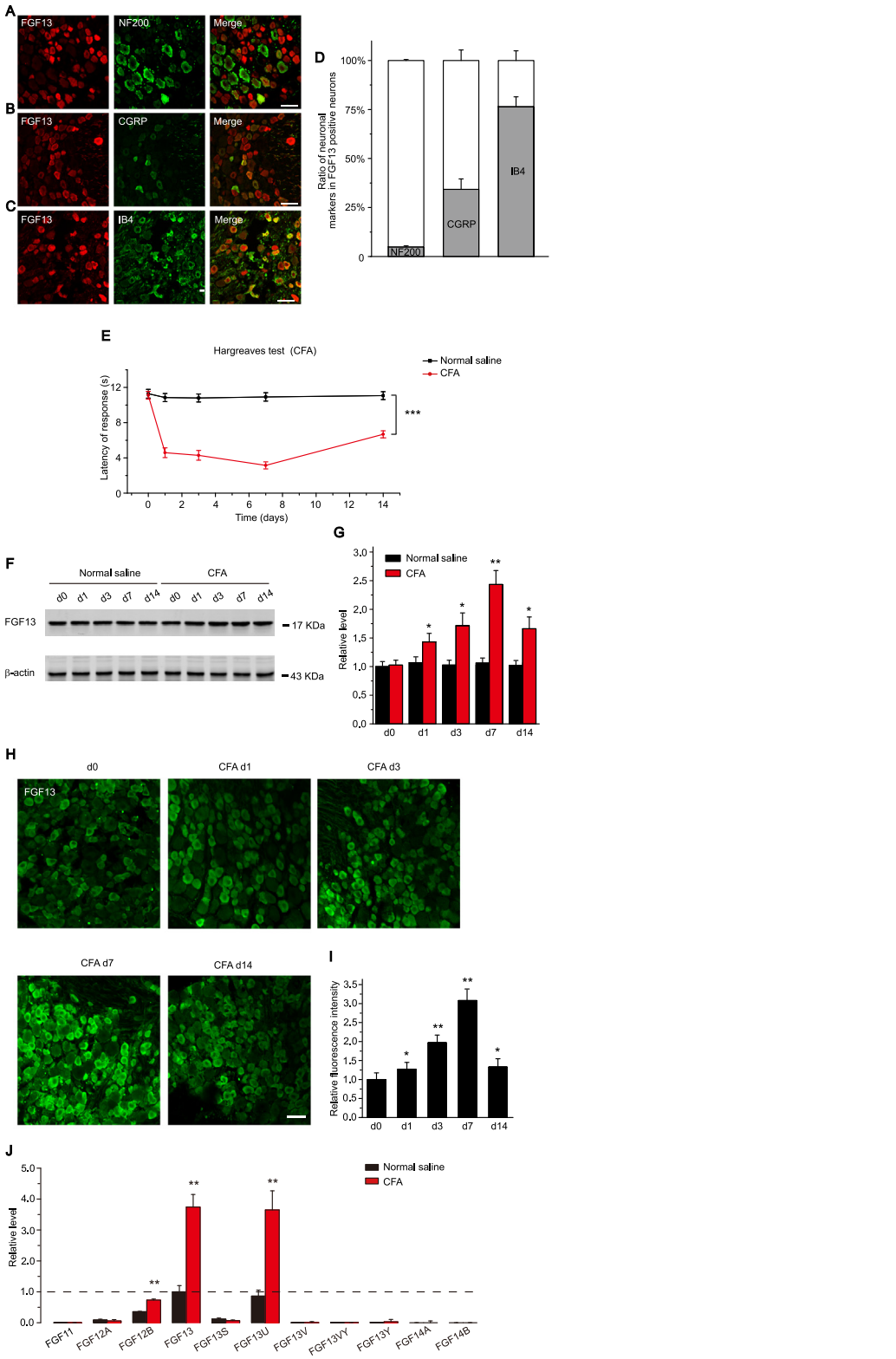

Fig. 2. CFA injection increased the expression of FGF13 in DRG neurons. (A, B, C) Representative immunofluorescence images depicted co-localization of FGF13 with different categories of neuronal markers in the DRG of wild type mice. NF200, a marker of large sized neurons; CGRP, a marker of small diameter peptidergic neurons; IB4, a marker of small diameter non-peptidergic neurons. (D) Quantification of overlap between FGF13 and neuronal markers. Scale bar: 50 μm. n = 3 mice/group. (E) Thermal pain hypersensitivity after intraplantar CFA injection in Loxp mice. n = 8 mice/group. (F) Representative images of FGF13 protein expression in L3-L5 DRGs on day 0, 1, 3, 7 and 14 after CFA or normal saline treatment detected by Western blot. (G) Summary of panel. (H) Representative immunofluorescence images of FGF13 labeled neurons in L4/L5 DRGs on day 0, 1, 3, 7 and 14 after CFA injection. Scale bar: 50 μm. (I) Summary of the relative fluorescence intensity of FGF13 staining. n = 3 mice/group. One-way ANOVA, followed by Dunnett's t *post hoc* test. (J) The relative expression levels of FGF11-14 in the ipsilateral L3-L5 DRGs on day 7 after CFA injection. All data were corrected with GAPDH and normalized to FGF13 of control group. $^{*}P < 0.05$, $^{**}P < 0.01$, $^{***}P < 0.001$.

Table 3
Summary of current-clamp properties of DRG cells.

	Loxp	KO	Loxp CFA	KO CFA
Cm (pF)	27.1 ± 1.6 (20)	28.2 ± 1.8 (20)	29.4 ± 1.8 (20)	29.9 ± 1.6 (20)
Rin (MΩ)	564.0 ± 48.4 (15)	485.7 ± 47.8 (15)	532.1 ± 47.1 (14)	474.7 ± 47.7 (17)
RMP (mV)	−58.1 ± 0.7 (15)	−58.7 ± 0.6 (17)	−60.3 ± 0.5 (17)	−59.4 ± 0.9 (15)
AP amplitude (mV)	107.4 ± 2.9 (16)	107.6 ± 3.0 (17)	105.2 ± 1.1 (16)	107.8 ± 2.4 (20)
Current threshold (pA)	132.1 ± 10.9 (20)	265.7 ± 34.1 (20)**	54.1 ± 8.2 (16)	142.1 ± 12.4 (20)##

The number of cells analyzed for each parameter is provided in parentheses.
** indicates p < 0.01, compared to Loxp group.
indicates p < 0.01, compared to Loxp CFA group.

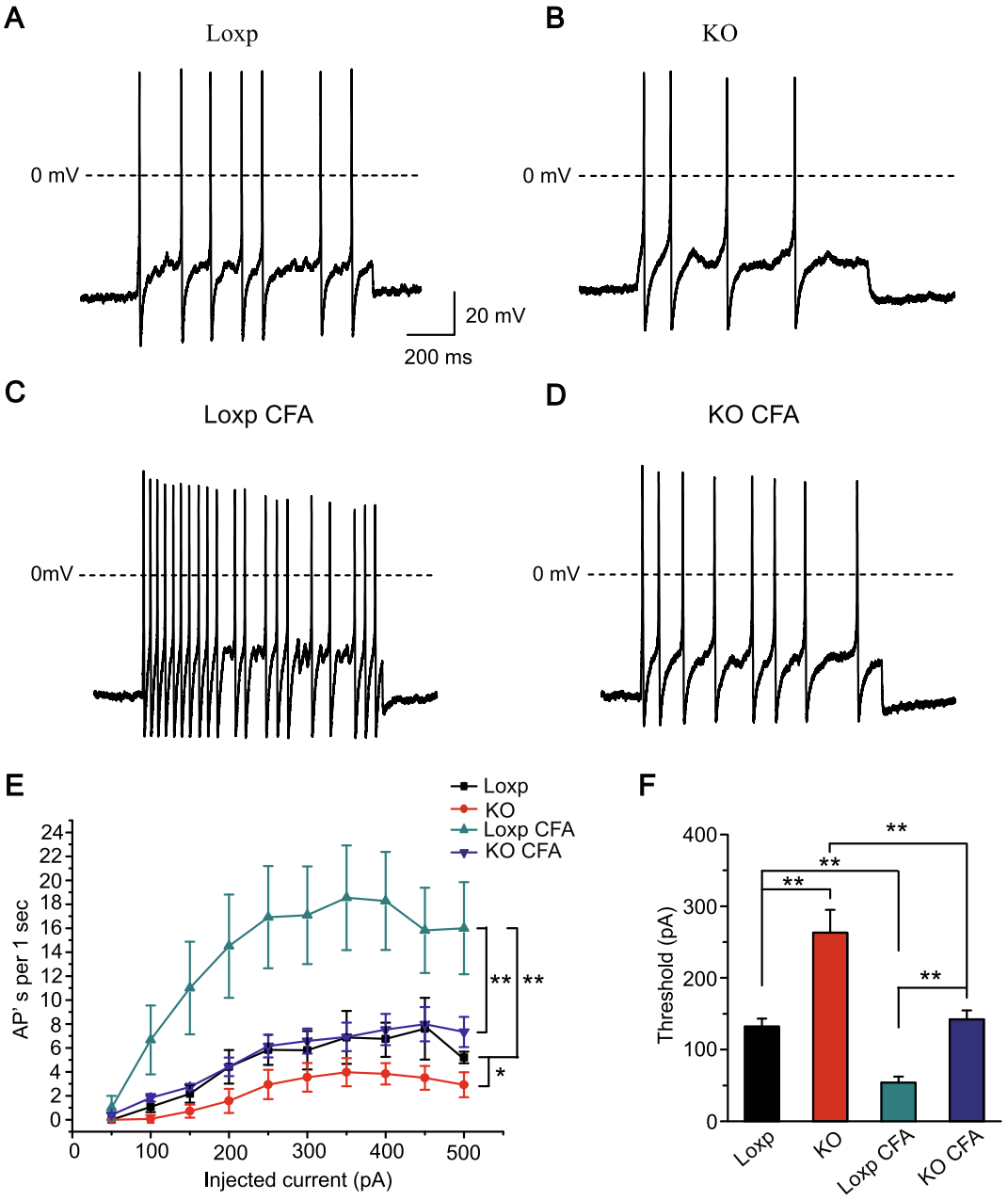

Fig. 3. *Fgf13* conditional knockout decreased the excitability of nociceptive DRG neurons. (A-D) Representative responses of DRG neurons from Loxp and KO mice to 1 s, 300pA depolarizing current injection. (E) The summary of the number of action potentials elicited by depolarizing current steps of neurons from KO mice and Loxp mice under either physiological or CFA-induced chronic inflammatory pain conditions. (F) The action potential threshold in small, current-clamped DRG neurons. n = 15–20 cells/group. One-way ANOVA, followed by Bonferroni *post hoc* test. $^{*}P < 0.05$, $^{**}P < 0.01$.

FGF13 was expressed predominantly in primary nociceptive small-diameter DRG neurons

We proceeded to examine FGF13 expression patterns in DRG neurons. Fig. 2A-C showed the representative immunofluorescence images depicting co-localization of FGF13 with different categories of neuronal markers, NF200, a marker of large-diameter neurons; IB4, a marker of small diameter non-peptidergic neurons and CGRP, a marker of small diameter peptidergic neurons [11,25]. Double-immunostaining showed that 4.9% ± 0.5% of FGF13 positive neurons expressed NF200 (Fig. 2A and D). In contrast, 34.3% ± 5.3% of FGF13 positive neurons expressed CGRP (Fig. 2B and D) and 76.5% ± 4.9% of FGF13 positive neurons expressed IB4 (Fig. 2C and D) in wild type mice. Therefore, the above results demonstrated that FGF13 was expressed predominantly in primary nociceptive small-diameter DRG neurons.

CFA treatment increased the expression of FGF13 in DRG neurons

We next examined the expression changes of FGF13 in CFA-induced inflammatory pain model. CFA-treated mice displayed significantly increased thermal hypersensitivity during 14 days of observation (Fig. 2E), consistent with previous studies [25]. We found that CFA treatment significantly increased the expression of FGF13 in ipsilateral L3-L5 DRGs at day1, 3, 7 and 14. The expression of FGF13 started to rise at day 1 and reached peak at day 7. For comparison, normal saline injection did not alter the level of FGF13 in L3-L5 DRGs during the observation period (Fig. 2F and G). We proceeded to examine FGF13 expression in DRG neurons by immunohistochemistry. Immunohistochemistry results showed that the expression of FGF13 in DRG neurons was increased after CFA treatment with the peak at day 7, consistent with our immunoblot results (Fig. 2H and I). CFA injection did not alter the expression of FGF13 in DRG neurons of KO mice (Suppl. Fig. 1A and B).

We further investigated the expression changes of FHF isoforms in mouse DRG tissues in CFA-induced inflammatory pain model. FGF13 has five isoforms, FGF13S (also known as FGF13A), FGF13U (also known as FGF13B), FGF13V, FGF13Y,FGF13VY [8]. qPCR results showed that FGF13U was the most abundant in the DRG (Fig. 2J and Suppl. Fig. 2). CFA treatment significantly increased the expression level of FGF13U. Transcript for FGF12B was also increased, but the expression levels of other FHF isoforms, including FGF13S showed no prominent change (Fig. 2J). Taken together, the above data suggest that FGF13 expression is markedly increased in ipsilateral DRG neurons during CFA-induced inflammatory pain.

Fgf13 conditional knockout attenuated CFA-induced hyper-excitability in DRG neurons

To explore whether FGF13 could affect DRG neuronal excitability, we investigated the firing properties of small-diameter DRG neurons via current clamp recording. There were no significant differences in input resistance, resting membrane potential and spike amplitude between *Fgf13*$^{-/Y}$ mice and control mice (Table 3). No spontaneous firing was detected with zero current injection. Representative traces of DRG neurons from Loxp and KO mice in response to 1 s, 300 pA depolarizing current injection are shown in Fig. 3A-D. When stimulated with step current injection, the frequency of repetitive firing during 1 s current steps of 50–500 pA injection was remarkably reduced in *Fgf13*$^{-/Y}$ mice compared with its controls. Moreover, 7 days post-CFA treatment, the total number of action potentials was decreased in KO mice compared with Loxp mice when the same amplitude of current was injected (Fig. 3E). Furthermore, under physiological conditions the current threshold needed to elicit the first action potential in DRG neurons was much higher in KO mice compared with Loxp mice. After CFA treatment, the current threshold was decreased in DRG neurons of Loxp mice, whereas conditional knockout of *Fgf13* potentiated CFA-induced current threshold decrease in DRG neurons of Loxp mice (Fig. 3F).

Fgf13 knockout attenuated CFA-induced increase in Na^+ currents in DRG neurons

Previous studies have shown that FGF13 has the capability of regulating Na^+ channels [8,11,27]. Therefore, we continued to explore whether FGF13 could regulate Na^+ current density and gating properties in DRG neurons under physiological and pathological conditions. We started by recording total Na^+ current evoked by a step depolarization in DRG neurons. To evaluate FGF13 mRNA expression in each DRG neuron recorded, each neuron was collected for single cell PCR after the patch-clamp recording. According to the single cell PCR results, we picked the FGF13 plus $Na_v1.8$ expression positive type ($FGF13^+/Na_v1.8^+$) from *Fgf13*$^{fl/Y}$ mice and $Na_v1.8$ positively expressed single neuron from *Fgf13*$^{-/Y}$ mice ($FGF13^-/Na_v1.8^+$) to analyze the neuronal Na^+ currents, respectively. Representative current traces are shown in Fig. 4A and B. The representative images of single cell PCR results are shown in Fig. 4C and D. We found that FGF13 deficiency reduced the amplitude of total Na^+ currents (Fig. 4E). To further investigate the effect of FGF13 on different subtypes of Na^+ currents, we used two sodium channel subtype selective inhibitors, TTX and ProTx-Ⅱ, to separate certain subtypes of Na^+ current. We found that the amplitude of TTX-S, TTX-R and $Na_v1.7$ sodium currents were all reduced after *Fgf13* deletion (Fig. 4F-H). Overall, these results showed that FGF13 deficiency reduced the amplitude of Na^+ current density. The amplitude reduction was observed in the current density of total, TTX-S, TTX-R and $Na_v1.7$ sodium channels (Fig. 4E-H). There were no differences in the gating properties of sodium channels, including the voltage dependence of activation (Suppl. Fig. 3A-D), steady state inactivation (Suppl. Fig. 3E-H) and the recovery from inactivation (Suppl. Fig. 3I) between $FGF13^-/Na_v1.8^+$ DRG neurons from *Fgf13*$^{-/Y}$ mice and the $FGF13^+/Na_v1.8^+$ controls from *Fgf13*$^{fl/Y}$ mice (Supplemental Table 1 and 2).

Further studies were conducted on mice under chronic inflammatory pain conditions. Na^+ currents in nociceptive DRG neurons were recorded at day 7 after CFA treatment. CFA injection potentiated the amplitude of total Na^+, TTX-S Na^+, TTX-R Na^+ and $Na_v1.7$ current density in Loxp mice DRG neurons. However, conditional knockout of *Fgf13* attenuated CFA-induced Na^+ current increase in DRG neurons of Loxp mice (Fig. 4E-H). Still, no changes were observed in the kinetics of Na^+ channels after CFA injection (Suppl. Fig. 4A-I, Supplemental Table 1 and 2). Therefore, the above results demonstrated that FGF13 was important for maintaining Na^+ channel activity without altering its gating properties.

FGF13 promoted the expression of Na^+ channels by interacting with and stabilizing microtubules

Previous studies showed that FGF13 deficiency resulted in a reduction in Na^+ current amplitude [8,11]. The reduction may be caused by reduced membrane Na^+ channel expression and/or changes in the gating properties. Having found no changes in the gating kinetics of Na^+ channels, we reckoned that the reduction in Na^+ current density in *Fgf13* KO DRG neurons might be caused by reduced membrane expression of Na^+ channels. Wu et al. showed that FGF13 could act as a microtubule-stabilizing protein [17] and microtubules form an important intracellular transport pathway to assist protein transport to the cell membrane [20,21]. We therefore hypothesize that FGF13 promotes sodium channel expression by regulating the stability of microtubules in DRG

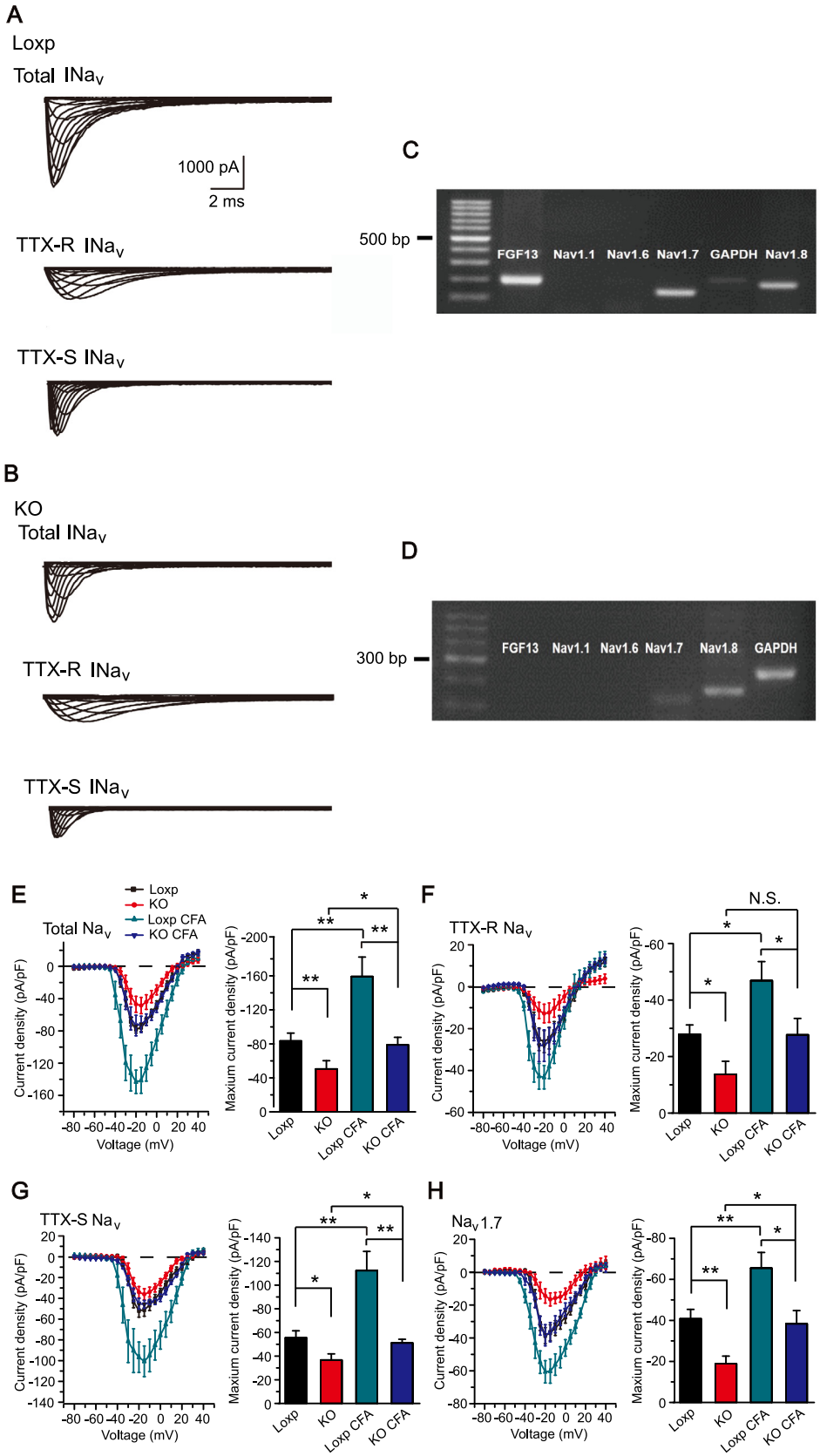

Fig. 4. *Fgf13* conditional knockout attenuated CFA-induced increase in Na^+ currents in DRG neurons. (A, B) Representative traces of total Na_v, TTX-R Na_v and TTX-S Na_v currents in $FGF13^+/Na_v1.8^+$ neurons of Loxp mice and $FGF13^-/Na_v1.8^+$neurons of KO mice. (C, D) Representative images of single cell PCR results. (E-H) Averaged current density of total Na_v, TTX-R Na_v, TTX-S Na_v and $Na_v1.7$ channels in L3-L5 DRG neurons 7 days after intraplantar CFA injection. n = 7–13 cells/group. One-way ANOVA, followed by Bonferroni *post hoc* test. $^*P < 0.05$, $^{**}P < 0.01$.

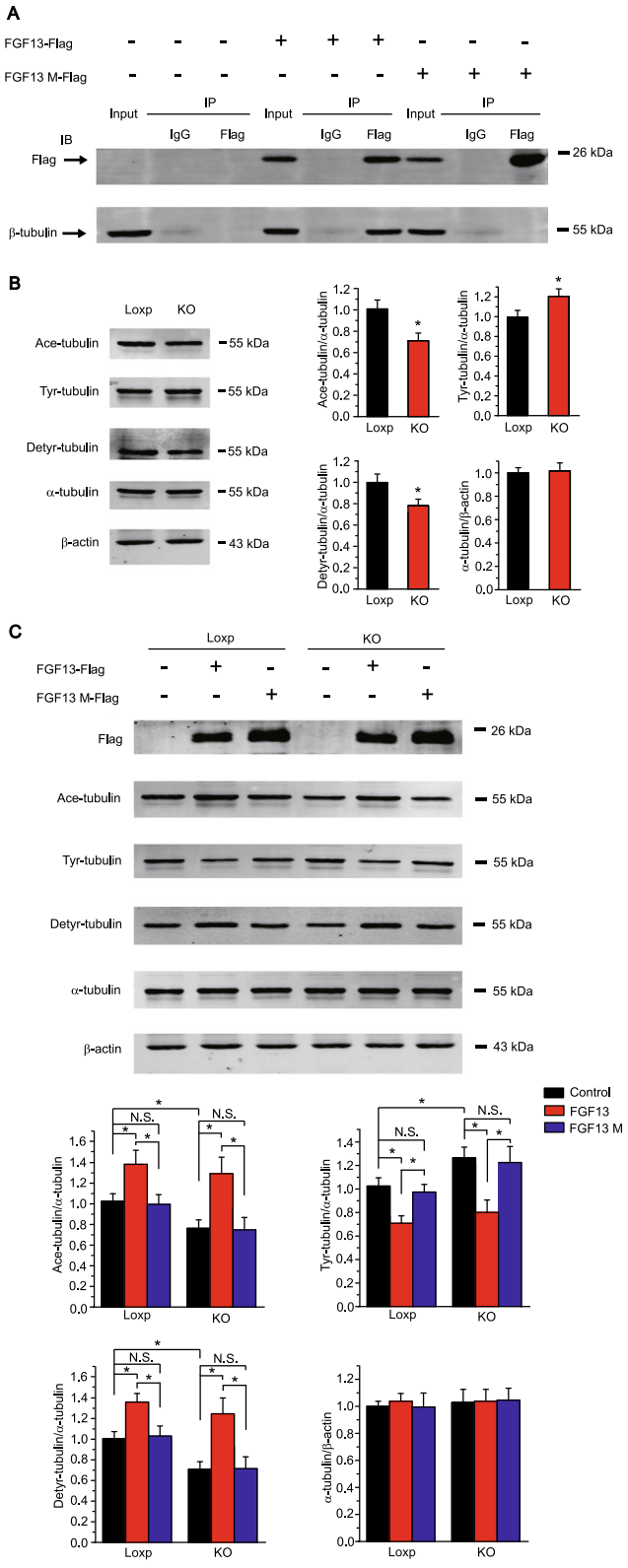

Fig. 5. FGF13 can modulate the stability of microtubules in DRG neurons. (A) The ability of FGF13 and FGF13 mutant to bind to tubulin was confirmed by co-IP. (B) Immunoblotting of DRG tissues showed the Ace-tubulin, Tyr-tubulin, Detyr-tubulinand α-tubulin levels in Loxp and KO mice. The lower panel showed the summarized data. n = 3 mice/group. (C) Western blots showed Ace-tubulin, Tyr-tubulin, Detyr-tubulin and α-tubulin expression in DRG neurons by overexpression of FGF13 or FGF13 mutant. The lower panel showed the summarized data. n = 3. 5 mice were included in each group. Two-way ANOVA, followed by Bonferroni *post hoc* test. $^{*}P < 0.05$.

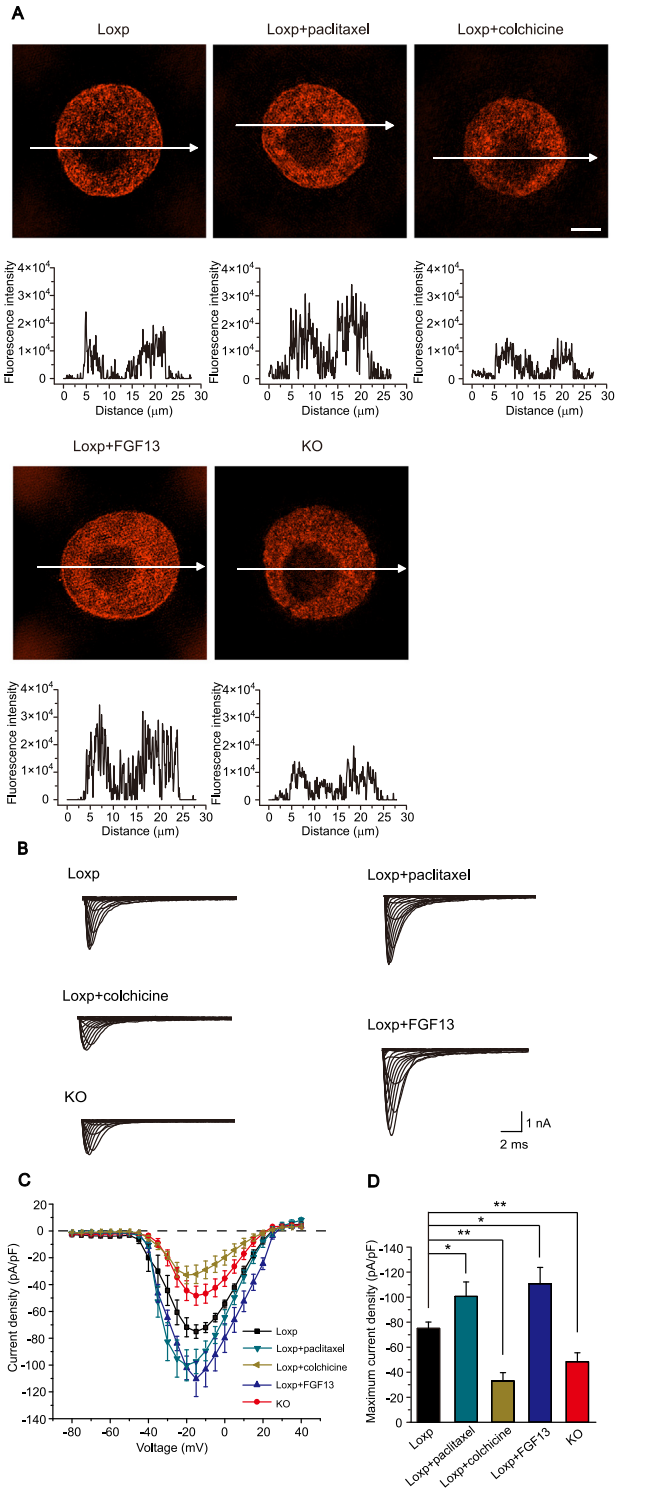

Fig. 6. The effect of pharmacological manipulation of microtubules on subcellular distribution of Na^+ channel proteins and Na^+ channel current density. (A) Subcellular localization of Na^+ channel proteins in different conditions. Scale bar: 5 μm. The lower panel showed the fluorescence intensities of Na^+ channel proteins along the line marked by the white arrow in the picture. (B) Representative Na^+ channel currents of DRG neurons. (C) I-V curves of Na^+ channel currents. (D) Maximum current density of Na^+ currents. n = 15–20 cells/group. One-way ANOVA, followed by Dunnett's t *post hoc* test. $^{*}P < 0.05$; $^{**}P < 0.01$.

neurons. We first tested whether FGF13 could interact with microtubules in DRG neurons. Previous studies have shown that $FGF13B^{S104\text{-}Q111}$ is the tubulin binding domain that mediates the

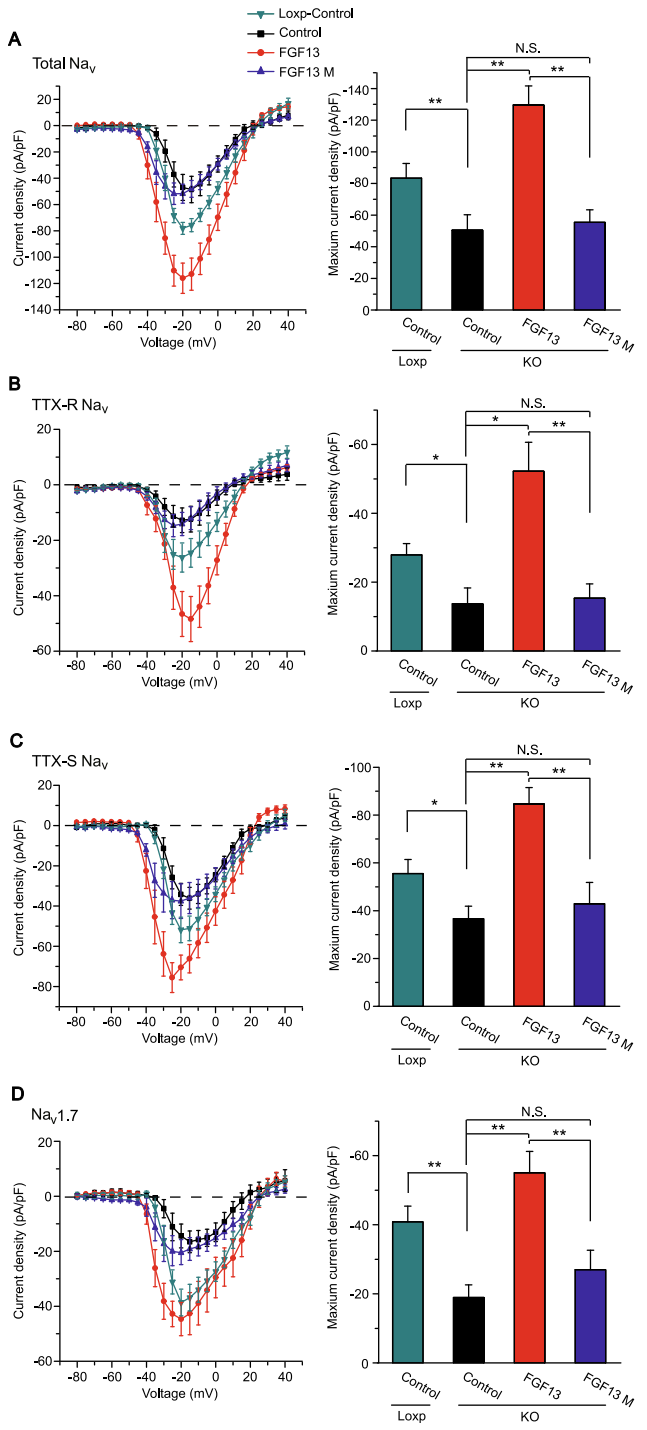

Fig. 7. FGF13 overexpression rescued the decrease in Na^+ channel current density in *Fgf13* conditional knockout mice. (A-D) Averaged current density of total Na_v, TTX-R Na_v, TTX-S Na_v and $Na_v1.7$ currents after the adenovirus-mediated delivery of FGF13 and FGF13 mutant (FGF13 M) in DRG neurons from KO mice. N = 7–16 cells/group. One-way ANOVA, followed by Bonferroni *post hoc* test. $^*P < 0.05$, $^{**}P < 0.01$.

binding of FGF13 to tubulin, and the mutant FGF13B$^{S104\text{-}Q111/104A\text{-}111A}$ is unable to interact with tubulin [17]. We then constructed a FGF13B adenoviral vector and FGF13B$^{S104\text{-}Q111/104A\text{-}111A}$ mutant (FGF13 mutant) adenoviral vector. We infected Flag-tagged FGF13 wild type and FGF13 mutant adenovirus in cultured DRG neurons of control mice, and co-IP assay showed that FGF13 directly interacted with tubulin, whereas the FGF13 mutant did not bind to tubulin (Fig. 5A). We further investigated whether FGF13 could act to stabilize microtubules in DRG neurons. Immunoblotting showed thatAce-tubulinand Detyr-tubulin, markers for stable microtubules [17,29], were reduced in DRG of *Fgf13* KO mice when compared with Loxp mice. Tyr-tubulin, a marker for dynamic microtubules, was increased in DRG of *Fgf13* KO mice when compared with Loxp mice. As a control, the expression of α-tubulin in the DRG was not altered in *Fgf13* KO group (Fig. 5B). This result suggested a reduction in the number of stable microtubules in *Fgf13* KO mice. We then infected FGF13 and FGF13 mutant adenovirus in cultured DRG neurons. Immunoblotting results demonstrated that FGF13, but not FGF13 mutant, up-regulated the expression of Ace-tubulin and Detyr-tubulin in Loxp mice. In addition, FGF13, but not FGF13 mutant, down-regulated the expression of Tyr-tubulin in Loxp mice. Similar results were observed in KO mice (Fig. 5C). The above results showed that in DRG neurons, FGF13 but not its mutant, increased acetylated tubulin expression, a marker of stable microtubules.

We next examined whether FGF13 could promote Na^+ channel expression and function through regulating the stability of microtubules in DRG neurons. We first tested whether pharmacological modulation of microtubule stability could affect the subcellular localization of Na^+ channel proteins. Treating DRG neurons with paclitaxel (20 μM), a known tubulin stabilizer, significantly enhanced the plasma membrane localization of Na^+ channel proteins in DRG neurons of Loxp mice. In contrast, treating DRG neurons with colchicine (20 μM), a known tubulin polymerization inhibitor, significantly reduced the expression of Na^+ channel proteins in the surface membrane (Fig. 6A). We then tested the effect of pharmacological modulation of microtubule stability on Na^+ channel activity. Treating DRG neurons with paclitaxel significantly enhanced the total Na^+ current density in Loxp mice. In contrast, treating DRG neurons with colchicine significantly reduced the total Na^+ current density in Loxp mice (Fig. 6B-D). We then overexpressed FGF13 in DRG neurons of Loxp mice via adenovirus infection. We found that FGF13 overexpression resulted in more Na^+ channel proteins being inserted into the surface membrane in Loxp mice, mimicking paclitaxel treatment. On the contrary, there was a decrease in surface membrane Na^+ channels expression following *Fgf13* knockout, similar to that of colchicine treatment (Fig. 6A). Voltage clamp recording showed a similar result. FGF13 overexpression resulted in an increase of total Na^+ current density in DRG neurons in Loxp mice, mimicking paclitaxel treatment. On the contrary, *Fgf13* knockout in DRG neurons resulted in reduced total Na^+ current density, mimicking colchicine treatment (Fig. 6B-D). In addition, we tested the subcellular localization of $Na_v1.7$ channel proteins in different conditions, and the immunocytochemistry results demonstrated a similar trend (Suppl. Fig. 4). These results suggest that the regulation of the stability of microtubules by FGF13 may be an important mechanism for translocation of Na^+ channels to the cell surface membrane in DRG neurons.

To further confirm the role of FGF13 in promoting Na^+ channel function through regulating the stability of microtubules in DRG neurons, we performed rescue experiments on DRG neurons of *Fgf13* KO mice by overexpression FGF13 and FGF13 mutant. FGF13 overexpression rescued the decrease of total Na^+ current density as well as its subtypes in KO mice, whereas no change in sodium current density was observed when FGF13 mutant was used to infect the FGF13-deficient DRG neurons (Fig. 7A-D).

Finally, to test whether the effect of FGF13 mutant on the sodium currents was due to lack of effect of FGF13 mutant on sodium currents in KO mice, we infected FGF13 and FGF13 mutant adenovirus in cultured DRG neurons of control mice and examined the binding properties. As shown in Suppl. Fig. 5, both FGF13 and FGF13 mutant could bind to sodium channels, suggesting that

Table 4
Summary of current-clamp properties of DRG cells.

		Cm (pF)	Rin (MΩ)	RMP (mV)	AP amplitude (mV)	CP (pA)
Loxp	control	28.1 ± 1.5 (21)	532.1 ± 40.1 (21)	−60.5 ± 0.9 (20)	112.4 ± 2.6 (22)	147.3 ± 9.7 (21)
	FGF13	28.7 ± 1.6 (21)	452.7 ± 25.9 (21)	−59.8 ± 0.8 (21)	109.9 ± 1.4 (21)	80.8 ± 8.2 (22)*
	FGF13 M	28.2 ± 1.7 (22)	426.4 ± 38.5 (22)	−59.9 ± 0.7 (20)	113.3 ± 2.4 (18)	148.4 ± 16.3 (23)
KO	control	31.8 ± 1.8 (20)	464.7 ± 41.7 (20)	−61.3 ± 1.0 (19)	109.5 ± 1.2 (19)	279.0 ± 23.4 (19)
	FGF13	31.2 ± 1.5 (23)	497.8 ± 12.3 (23)	−61.5 ± 0.7 (19)	113.9 ± 1.4 (20)	144.2 ± 20.7 (20)##
	FGF13 M	32.0 ± 1.4 (19)	482.9 ± 22.5 (19)	−61.3 ± 1.2 (19)	111.3 ± 1.8 (21)	270.4 ± 20.5 (20)

The number of cells analyzed for each parameter is provided in parentheses.
* indicates $p < 0.05$, compared to Loxp control group.
indicates $p < 0.01$, compared to KO control group.

the effect of FGF13 mutant on the sodium currents in KO mice was due to the lack of the binding ability to tubulin, but not to sodium channels. Taken together, these results support the view that FGF13 could stabilize microtubules and thereby modulate sodium channel membrane expression in small-diameter DRG neurons.

FGF13 increased the excitability of small-diameter nociceptive DRG neurons by stabilizing microtubules

Having established that FGF13 promotes the expression of Na^+ channels by stabilizing microtubules, we hypothesized that FGF13 would have measureable effects on the excitability of small-diameter nociceptive DRG neurons by stabilizing microtubules. We recorded the firing properties by FGF13 or FGF13 mutant overexpression in Loxp or *Fgf13* KO DRG neurons. There were no significant differences in input resistance, resting membrane potential or spike amplitude after FGF13 or FGF13 mutant overexpression in Loxp or *Fgf13* KO DRG neurons (Table 4). FGF13 overexpression increased the excitability either in Loxp or *Fgf13* KO nociceptor DRG neurons. In contrast, the neuronal excitability was not altered upon FGF13 mutant overexpression (Fig. 8A-L) Moreover, in *Fgf13* KO mice, the frequency of repetitive firing for 1 s current steps of 50–500 pA was remarkably increased after FGF13 overexpression, while FGF13 mutant overexpression did not change the neuronal firing frequency (Fig. 8G and H). Meanwhile, the current threshold to elicit the first action potential was decreased in KO mice after FGF13 overexpression, while FGF13 mutant overexpression did not change the current threshold (Fig. 8I). To further confirm the effect of FGF13 on neuronal excitability in *Fgf13* knockout mice, a linear ramp current was applied to measure action potential firing parameters. After FGF13 overexpression, the action potential threshold elicited by ramp current stimulation was decreased in small-diameter DRG neurons (Fig. 8E and K). Meanwhile, the number of action potentials was increased (Fig. 8J and L). However, the FGF13 mutant did not change the firing properties compared with the control group. This was consistent with the results of step current injection stimulation. These data indicate that FGF13 enhances the excitability of small-diameter DRG neurons via stabilizing microtubules. Taken together, FGF13 overexpression clearly rescued the decreased electrophysiological deficits, which suggesting that FGF13 is an important factor regulating sodium channels and neuronal excitability.

Discussion

This study showed that *Fgf13* conditional knockout mice exhibited reduced nocifensive responses to inflammatory pain. FGF13 was expressed predominantly in small-diameter DRG neurons and CFA injection increased the expression of FGF13 in the DRG. FGF13 deficiency resulted in a reduction in sodium current amplitude. Furthermore, stabilized microtubules were increased in DRG neurons by the overexpression of FGF13, but not FGF13 mutant, which lacks tubulin binding capability. FGF13 overexpression rescued the decreased sodium currents and neuronal excitability in *Fgf13* KO mice, whereas FGF13 mutant did not. This study demonstrated that FGF13 could modulate inflammatory pain by stabilizing microtubules to promote sodium channel function and excitability in small-diameter nociceptive DRG neurons.

Following peripheral inflammation, changes in the expression profiles of growth factors in primary afferent neurons may contribute to the development of chronic inflammatory pain. A previous study reported that among the FGF family, the array signals for FGF13 were markedly altered in rat DRG after peripheral nerve injury [30]. After CFA treatment, FGF12B and FGF13 were up-regulated. The results indicated that, in addition to FGF13, FGF12 might also be involved in the response of DRG neurons to inflammatory pain, which may need further study.

It has been reported that FGF13 was expressed in neurons, but not in glial cells or other types of cells in the DRG [7,30]. Consistent with this, we found that FGF13 was expressed exclusively in neuronal cells and mainly in primary nociceptive small-diameter neurons in the DRG. Furthermore, we found that FGF13U was the most abundant among FGF13 isoforms in the DRG. The level of mRNA for FGF13S was detectable, but at much lower levels compared with FGF13U. More importantly, CFA treatment markedly increased the expression of FGF13U but not FGF13S. The data indicates that FGF13U may play an important role in CFA-induced chronic inflammatory pain. It has been demonstrated that overexpression of FGF13S and FGF13U can differentially modulate voltage-gated sodium channel activity in heterologous expression systems [27]. Therefore, it will be interesting to explore the roles of other isoforms of FGF13 in the DRG in future studies.

In the present study we found that CFA treatment increased the sodium currents and neuronal excitability in DRG neurons of Loxp mice. However, *Fgf13* knockout could only partially attenuate the up-regulation of sodium channels and the increase of neuronal excitability induced by CFA injection. We excluded the possibility that CFA treatment might increase the expression of FGF13 in *Fgf13* knockout mice. Therefore, these data suggested that there might be some other mechanisms participating in the modulation of sodium channels and neuronal excitability in $Fgf13^{-/Y}$ mice after CFA treatment, in addition to the mechanism that FGF13 stabilizes microtubules to promote sodium channel function. For example, CFA treatment can induce the release of inflammatory mediators, such as IL-1β and TNF-α [3] in local inflamed tissues, which upregulated the expression and function of sodium channels via various mechanisms (post-translational modifications, trafficking regulation including microtubule mediated transport, etc.) and further regulated the excitability of DRG neurons [4,5,6,31].

It has been reported that FGF13 knockdown in mouse ventricular myocytes decreased the expression of $Na_v1.5$ at sarcolemma [8], suggesting that FGF13 might affect the trafficking of sodium

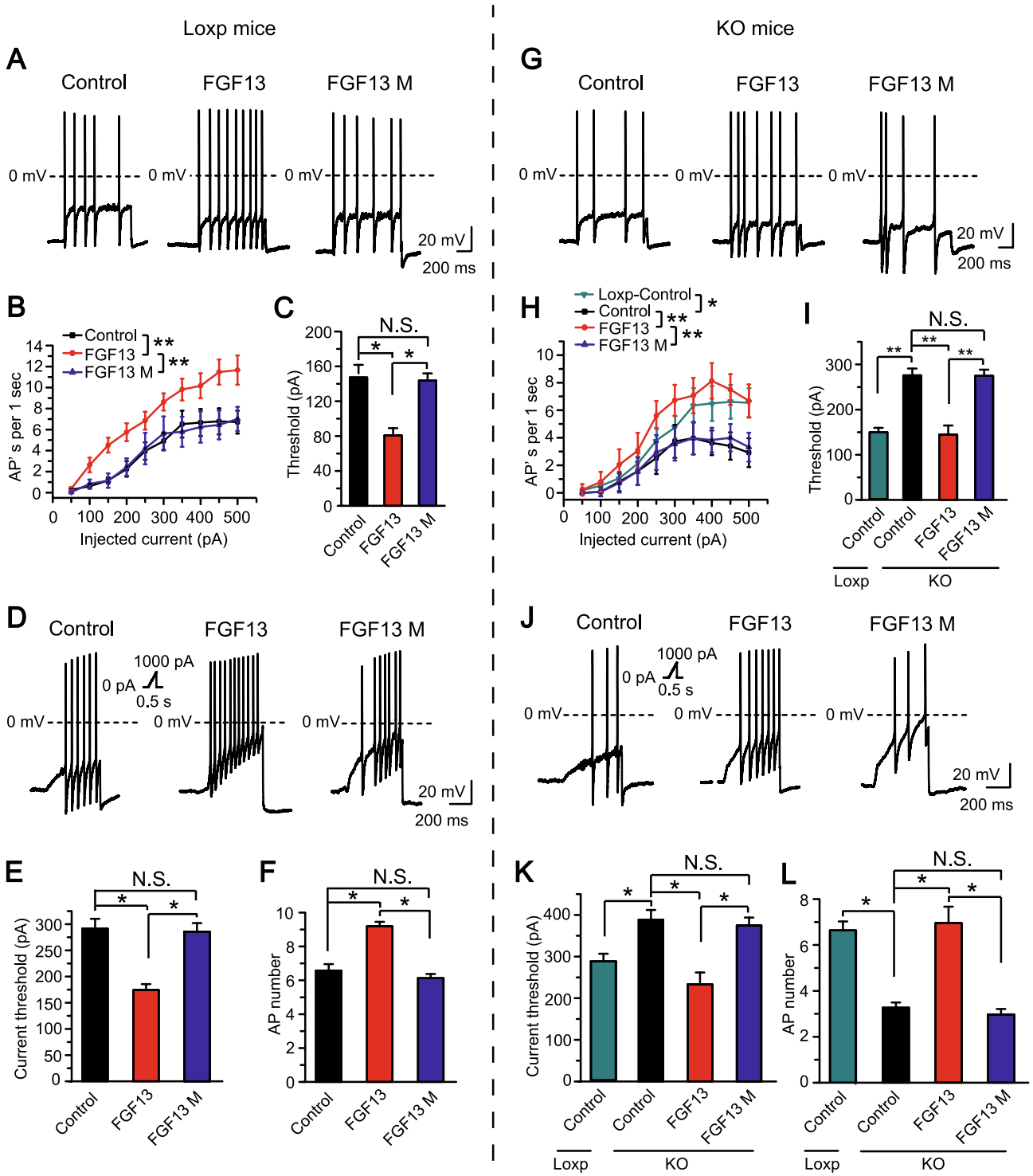

Fig. 8. FGF13 overexpression rescued the decreased excitability of *Fgf13* conditional knockout mice. (A, G) Representative response of DRG neurons from Loxp and KO mice to 1 s, 300pA depolarizing current injection. (B, H) Summary of the number of action potentials elicited by depolarizing current steps in DRG neurons. Current steps start from 50 to 500 pA, with 50 pA increment, lasting 1 s. (C, I) Summary of the current threshold for eliciting action potentials in DRG neurons. One-way ANOVA, followed by Bonferroni *post hoc* test. (D, J) Representative current clamp recordings of three groups in DRG neurons under ramp current stimulation from 0 to 1000 pA of 500 ms duration (see inset). (E, K) Summary of the action potential threshold in small, current-clamped DRG neurons elicited by ramp current stimulation. One-way ANOVA, followed by Bonferroni *post hoc* test. (F, L) Summary of the number of action potentials elicited by ramp current stimulation. n = 15–24 cells/group. One-way ANOVA, followed by Bonferroni *post hoc* test. $^{*}P < 0.05$, $^{**}P < 0.01$.

channels. The present study found that FGF13 could promote the expression and function of sodium channels by interacting with and stabilizing microtubules in DRG neurons, which provided novel mechanistic insights into how FGF13 regulated sodium channel trafficking. However, we cannot exclude other mechanisms involved in the regulation of sodium channels by FGF13. FHFs have been reported to bind to a neuronal MAPK scaffold protein, isletbrain-2 (IB2). FHFs could act as cofactors to recruit p38δ MAPK to IB2 to participate in MAPK signaling [7,32]. Several studies have reported that site-specific phosphorylation of Na_v α subunits by

p38 MAP kinase could modulate sodium channel properties [33,34]. Therefore, it might be interesting to explore whether FGF13 could also modulate sodium channel through p38 MAPK dependent mechanism.

Conclusion

FGF13 was expressed predominantly in small-diameter nociceptive DRG neurons, and the expression of FGF13 was up-regulated in CFA-induced chronic inflammatory pain condition. The study analyzed the expression changes of FHF isoforms in the DRG in CFA-induced inflammatory pain. FGF13 stabilized microtubules to modulate sodium channel function and the excitability of nociceptive neurons, therefore modulate inflammatory pain. However, further studies are needed to define the effect of FGF13 isoforms in inflammatory pain regulation. The study provided behavioral evidence and molecular mechanism for the contribution of FGF13 to inflammatory pain. Our study suggests that FGF13 may represent a novel therapeutic target in the treatment of inflammatory pain.

CRediT authorship contribution statement

Qiong Wang: Methodology, Validation, Investigation, Visualization, Writing - original draft. **Jing Yang:** Methodology, Validation, Investigation, Visualization, Writing - original draft. **Handong Wang:** Methodology, Validation, Investigation, Visualization, Writing - original draft. **Bin Shan:** Methodology, Validation, Investigation. **Chengyu Yin:** Methodology, Validation, Investigation. **Hang Yu:** Methodology, Validation, Investigation. **Xuerou Zhang:** Methodology, Validation, Investigation. **Zishan Dong:** Methodology, Validation, Investigation. **Yulou Yu:** Methodology, Validation, Investigation. **Ran Zhao:** Methodology, Validation, Investigation. **Boyi Liu:** Conceptualization, Writing - original draft, Writing - review & editing. **Hailin Zhang:** Conceptualization, Writing - original draft, Writing - review & editing. **Chuan Wang:** Conceptualization, Writing - original draft, Supervision, Writing - review & editing.

Declaration of Competing Interest

The authors declare that they have no known competing financial interests or personal relationships that could have appeared to influence the work reported in this paper.

Acknowledgements

This work was supported by the National Natural Science Foundation of China (No.81770407, No.31171097, No.81900249, No.81873365, No.81603676), the Natural Science Foundation of Hebei Province (No.H2017206262, No.C2018206277), the Research Project of Science and Technology of High School of Hebei Province (No.ZD2015007, No.ZD2016002), the High-level Talent Support Project Hebei Province (No.A2017005070, No.A201901032), Zhejiang Provincial Natural Science Funds for Distinguished Young Scholars (No.LR17H270001), the College Students Innovative Pilot Project in Hebei Medical University (USIP2018048), Innovation Subsidy Project for Postgraduates in Higher Education Institutions of Hebei Provincial Education Department (CXZZBS2019113). We thank Alice Gregorie for the helpful comments on the manuscript. Q. Wang, J. Yang and H. Wang contributed equally to this work. C. Wang, H. Zhang and B. Liu are joint corresponding authors.

Appendix A. Supplementary data

Supplementary data to this article can be found online at https://doi.org/10.1016/j.jare.2020.12.009.

References

[1] Cummins TR, Sheets PL, Waxman SG. The roles of sodium channels in nociception: Implications for mechanisms of pain. Pain 2007;131(3):243–57.
[2] Dib-Hajj SD, Cummins TR, Black JA, Waxman SG. Sodium channels in normal and pathological pain. Annu Rev Neurosci 2010;33:325–47.
[3] Caceres AI, Liu B, Jabba SV, Achanta S, Morris JB, Jordt SE. Transient Receptor Potential Cation Channel Subfamily M Member 8 channels mediate the anti-inflammatory effects of eucalyptol. Br J Pharmacol 2017;174(9):867–79.
[4] Ding HH, Zhang SB, Lv YY, Ma C, Liu M, Zhang KB, et al. TNF-alpha/STAT3 pathway epigenetically upregulates Nav1.6 expression in DRG and contributes to neuropathic pain induced by L5-VRT. Journal of neuroinflammation 2019;16(1):29.
[5] He XH, Zang Y, Chen X, Pang RP, Xu JT, Zhou X, et al. TNF-alpha contributes to up-regulation of Nav1.3 and Nav1.8 in DRG neurons following motor fiber injury. Pain 2010;151(2):266–79.
[6] Noh MC, Stemkowski PL, Smith PA. Long-term actions of interleukin-1beta on K(+), Na(+) and Ca(2+) channel currents in small, IB4-positive dorsal root ganglion neurons; possible relevance to the etiology of neuropathic pain. J Neuroimmunol 2019;332:198–211.
[7] Goldfarb M. Fibroblast growth factor homologous factors: evolution, structure, and function. Cytokine Growth Factor Rev 2005;16(2):215–20.
[8] Wang C, Hennessey JA, Kirkton RD, Wang C, Graham V, Puranam RS, et al. Fibroblast growth factor homologous factor 13 regulates Na+ channels and conduction velocity in murine hearts. Circ Res 2011;109(7):775–82.
[9] Pablo JL, Wang C, Presby MM, Pitt GS. Polarized localization of voltage-gated Na+ channels is regulated by concerted FGF13 and FGF14 action. PNAS 2016;113(19):E2665–74.
[10] Yan H, Pablo JL, Wang C, Pitt GS. FGF14 modulates resurgent sodium current in mouse cerebellar Purkinje neurons. eLife 2014;3:e04193.
[11] Yang L, Dong F, Yang Q, Yang PF, Wu R, Wu QF, et al. FGF13 Selectively Regulates Heat Nociception by Interacting with Nav1.7. Neuron 2017;93(4):806–821 e809.
[12] Hennessey JA, Marcou CA, Wang C, Wei EQ, Wang C, Tester DJ, et al. FGF12 is a candidate Brugada syndrome locus. Heart rhythm 2013;10(12):1886–94.
[13] Wang X, Tang H, Wei EQ, Wang Z, Yang J, Yang R, et al. Conditional knockout of Fgf13 in murine hearts increases arrhythmia susceptibility and reveals novel ion channel modulatory roles. J Mol Cell Cardiol 2017;104:63–74.
[14] Wei EQ, Sinden DS, Mao L, Zhang H, Wang C, Pitt GS. Inducible Fgf13 ablation enhances caveolae-mediated cardioprotection during cardiac pressure overload. PNAS 2017;114(20):E4010–9.
[15] Gecz J, Baker E, Donnelly A, Ming JE, McDonald-McGinn DM, Spinner NB, et al. Fibroblast growth factor homologous factor 2 (FHF2): gene structure, expression and mapping to the Borjeson-Forssman-Lehmann syndrome region in Xq26 delineated by a duplication breakpoint in a BFLS-like patient. Hum Genet 1999;104(1):56–63.
[16] Wang Q, Bardgett ME, Wong M, Wozniak DF, Lou J, McNeil BD, et al. Ataxia and paroxysmal dyskinesia in mice lacking axonally transported FGF14. Neuron 2002;35(1):25–38.
[17] Wu QF, Yang L, Li S, Wang Q, Yuan XB, Gao X, et al. Fibroblast growth factor 13 is a microtubule-stabilizing protein regulating neuronal polarization and migration. Cell 2012;149(7):1549–64.
[18] Argyriou AA, Kyritsis AP, Makatsoris T, Kalofonos HP. Chemotherapy-induced peripheral neuropathy in adults: a comprehensive update of the literature. Cancer management and research 2014;6:135–47.
[19] Carlson K, Ocean AJ. Peripheral neuropathy with microtubule-targeting agents: occurrence and management approach. Clinical breast cancer 2011;11(2):73–81.
[20] Poulain FE, Sobel A. The microtubule network and neuronal morphogenesis: Dynamic and coordinated orchestration through multiple players. Molecular and cellular neurosciences 2010;43(1):15–32.
[21] Witte H, Bradke F. The role of the cytoskeleton during neuronal polarization. Curr Opin Neurobiol 2008;18(5):479–87.
[22] Agarwal N, Offermanns S, Kuner R. Conditional gene deletion in primary nociceptive neurons of trigeminal ganglia and dorsal root ganglia. Genesis 2004;38(3):122–9.
[23] Zheng X, Tai Y, He D, Liu B, Wang C, Shao X, et al. ETAR and protein kinase A pathway mediate ET-1 sensitization of TRPA1 channel: A molecular mechanism of ET-1-induced mechanical hyperalgesia. Molecular pain 2019;15:1744806919842473
[24] Yin C, Liu B, Wang P, Li X, Li Y, Zheng X, et al. Eucalyptol alleviates inflammation and pain responses in a mouse model of gout arthritis. Br J Pharmacol 2020;177(9):2042–57.
[25] Wang Y, Gao Y, Tian Q, Deng Q, Wang Y, Zhou T, et al. TRPV1 SUMOylation regulates nociceptive signaling in models of inflammatory pain. Nat Commun 2018;9(1):1529.
[26] Hu Q, Wang Q, Wang C, Tai Y, Liu B, Shao X, et al. TRPV1 Channel Contributes to the Behavioral Hypersensitivity in a Rat Model of Complex Regional Pain Syndrome Type 1. Front Pharmacol 2019;10:453.

[27] Yang J, Wang Z, Sinden DS, Wang X, Shan B, Yu X, et al. FGF13 modulates the gating properties of the cardiac sodium channel Nav1.5 in an isoform-specific manner. Channels 2016;10(5):410–20.
[28] Schmalhofer WA, Calhoun J, Burrows R, Bailey T, Kohler MG, Weinglass AB, et al. ProTx-II, a selective inhibitor of NaV1.7 sodium channels, blocks action potential propagation in nociceptors. Mol Pharmacol 2008;74(5):1476–84.
[29] Roll-Mecak A. How cells exploit tubulin diversity to build functional cellular microtubule mosaics. Curr Opin Cell Biol 2019;56:102–8.
[30] Li GD, Wo Y, Zhong MF, Zhang FX, Bao L, Lu YJ, et al. Expression of fibroblast growth factors in rat dorsal root ganglion neurons and regulation after peripheral nerve injury. NeuroReport 2002;13(15):1903–7.
[31] Binshtok AM, Wang H, Zimmermann K, Amaya F, Vardeh D, Shi L, et al. Nociceptors are interleukin-1beta sensors. The Journal of neuroscience : the official journal of the Society for Neuroscience 2008;28(52):14062–73.
[32] Schoorlemmer J, Goldfarb M. Fibroblast growth factor homologous factors are intracellular signaling proteins. Current biology : CB 2001;11(10):793–7.
[33] Hudmon A, Choi JS, Tyrrell L, Black JA, Rush AM, Waxman SG, et al. Phosphorylation of sodium channel Na(v)1.8 by p38 mitogen-activated protein kinase increases current density in dorsal root ganglion neurons. The Journal of neuroscience : the official journal of the Society for Neuroscience 2008;28(12):3190-3201.
[34] Wittmack EK, Rush AM, Hudmon A, Waxman SG, Dib-Hajj SD. Voltage-gated sodium channel Nav1.6 is modulated by p38 mitogen-activated protein kinase. The Journal of neuroscience : the official journal of the Society for Neuroscience 2005;25(28):6621-6630.